Journal of Neuroscience Methods 187 (2010) 41–45

Contents lists available at ScienceDirect

Journal of Neuroscience Methods

journal homepage: www.elsevier.com/locate/jneumeth

High resolution stereoscopic volume visualization of the mouse arginine vasopressin system

R.J. Clements*, E.M. Mintz, J.L. Blank

Department of Biological Sciences, Kent State University, Kent, OH 44242, USA

ARTICLE INFO

Article history:
Received 19 October 2009
Received in revised form
10 December 2009
Accepted 11 December 2009

Keywords:
Vasopressin
Anatomy
Stereoscopic
Visualization
Hypothalamus
Reconstruction

ABSTRACT

New imaging technologies have increased our capabilities to resolve three-dimensional structures from microscopic samples. Laser-scanning confocal microscopy is particularly amenable to this task because it allows the researcher to optically section biological samples, creating three-dimensional image volumes. However, a number of problems arise when studying neural tissue samples. These include data set size, physical scanning restrictions, volume registration and display. To deal with these issues, we undertook large-scale confocal scanning microscopy in order to visualize neural networks spanning multiple tissue sections. We demonstrate a technique to create and visualize a three-dimensional digital reconstruction of the hypothalamic arginine vasopressin neuroendocrine system in the male mouse. The generated three-dimensional data included a volume of tissue that measures 4.35 mm × 2.6 mm × 1.4 mm with a voxel resolution of 1.2 μm. The dataset matrix included 3508 × 2072 × 700 pixels and was a composite of 19,600 optical sections. Once reconstructed into a single volume, the data is suitable for interactive stereoscopic projection. Stereoscopic imaging provides greater insight and understanding of spatial relationships in neural tissues' inherently three-dimensional structure. This technique provides a model approach for the development of data sets that can provide new and informative volume rendered views of brain structures. This study affirms the value of stereoscopic volume-based visualization in neuroscience research and education, and the feasibility of creating large-scale high resolution interactive three-dimensional reconstructions of neural tissue from microscopic imagery.

1. Introduction

With the technological advancement of both imaging and display technologies, large-scale three-dimensional (3D) imaging has become a viable form of data sampling. Imaging techniques from MRI to confocal microscopy produce large datasets composed of individual image slices that combine to form a volume with three dimensions. These volumes can be reconstructed and visualized (Liu et al., 1997). New advances in computer hardware and software allow the rendering of moderately sized image volumes in real time at interactive frame rates. By merging software and hardware-based techniques, the generated data can be viewed in true stereoscopic 3D in which different viewpoints of the object are directed towards each eye. Our brain then reproduces information regarding 3D shape and depth using the optical disparity between each viewpoint (Orban et al., 2006). This generates a 3D perception of the object, immersing the user in the data environment that facilitates exploration and analysis. Indeed, stereoscopic imaging has proven to increase surgical accuracy (Thomsen and Lang, 2004) and stereoscopy is a valuable tool for augmented reality applications (Birkfellner et al., 2003), teaching (Perry et al., 2007; Sheen et al., 2004) and microscopy (Liao et al., 1997; Smith et al., 1999). While display hardware/software continues to evolve, the ability to generate massive high resolution datasets is ahead of these display capabilities. For this reason, the generation and display of high resolution data is an active research topic that spans disciplines and has recognized utility. For example, large-scale high resolution microscopic imaging allows the preservation of fine details while maintaining larger scale functional anatomy. One of the major goals of the study of neuroscience is to understand how individual neurons interact and function at the level of the network. Conventional confocal microscopy allows the imaging of individual tissue sections with thicknesses at most between 100 and 200 μm, but many nuclei or neuronal connections span millimeter distances through the tissue. Typically, researchers image individual sections of tissue and infer the 3D structure from sequential slices. The goal of the present study was to investigate the validity and usefulness of recombining multiple optically sectioned brain slices and microscopic fields into a single 3D volume representative of a larger piece of tissue.

To test this methodology, we chose to map the arginine vasopressin (AVP) neuronal system in male mice to create a high resolution 3D anatomical reconstruction of the anterior hypotha-

* Corresponding author at: Department of Biological/Biomedical Sciences, A311A Cunningham Hall, Kent State University, Kent, OH 44224, USA. Tel.: +1 330 672 2984.
E-mail address: rclement@kent.edu (R.J. Clements).

0165-0270/$ – see front matter © 2009 Elsevier B.V. All rights reserved.
doi:10.1016/j.jneumeth.2009.12.011

lamus. AVP is involved in body fluid homeostasis by regulating renal water filtration, as well as the regulation of social behavior (McCormick and Bradshaw, 2006; Caldwell et al., 2008). In the anterior hypothalamus, vasopressin is mainly released from neurons of the supraoptic and paraventricular nuclei. Vasopressin is regulated by a number of factors including angiotensin II, hyperosmolarity, and sympathetic stimulation (Stricker and Verbalis, 1999), as well as the behavioral state of the animal (Caldwell et al., 2008). We undertook large-scale confocal scanning of hypothalamic regions containing immunoreactive vasopressin and merged data sets from microscopic fields and physical slices to create a three-dimensional map of a portion of the mouse vasopressin system, and assessed its suitability for stereoscopic volume rendering.

2. Materials and Methods

2.1. Animals

Two, 4-month-old male mice (CF-1 strain) purchased from Charles River (Wilmington, MA.) were used for the procedure. Mice were housed individually with food and water, *ad libitum* and maintained on a 12L:12D light cycle (lights on at 0730). Temperature and humidity in the vivarium were maintained at 22 °C and 72%, respectively until processing.

2.2. Tissue processing

Animals were given CO_2 pre-treatment followed by rapid decapitation and brain removal. Brains were placed for 24 h in 4% para-formaldehyde followed by phosphate buffered saline (PBS) pH 7.0 until slicing. Brains were sliced on a media cooled vibratome at 200 μm per slice. A total of seven consecutive tissue sections were used for the staining procedure that included the hypothalamic vasopressin system (including the paraventricular (PVN), suprachiasmatic (SCN) and supraoptic nucleus (SON)). Slices were stored in PBS in a multi-well plate at 4°.

2.3. Fluorescent staining

The immunohistochemical staining procedure utilized a double antibody approach. Initially, the tissue sections were incubated in 3% normal horse serum, PBS, 0.5% triton X-100 for 24 h to block non-specific binding and permeabilize the tissue. After three washes (20 min each) in PBS, the sections were incubated in primary antibody (rabbit anti-vasopressin 1:250 (Chemicon)) for 3 days. After 3, 20 min washes in PBS the slices were incubated for 48 h in the secondary antibody (horse anti-rabbit IgG texas red (Molecular Probes) 1:500). Finally, the sections were washed a further 3 times (20 min each) and coverslipped under vectashield mounting media (Molecular Probes), sealed with clear nail polish, and refrigerated until microscopically imaged.

2.4. Microscopy

An Olympus FV 500 confocal microscope with four laser lines and motorized XYZ stage was used to acquire all data. Seven 200 μm-thick brain sections were excited with the HENE 560 laser line and fluorescence signal acquired using a 20X objective. To scan the individual sections containing the regions of interest, a program was generated using Olympus' stage management software (Programmable Acquisition Protocol Processor, PAPP) to manipulate the automated stage and acquire an array of image stacks from each physical section. The region of interest included 28 microscopic fields per section that were arranged in a grid that was 7 fields wide and 4 microscopic fields high. An image stack was captured from each of the 28 microscopic fields per slice that would later be recombined. Each image stack contained 100 optical sections with a resolution of 512 pixels × 512 pixels per image section. The program required human intervention to select the next microscopic field, as well as save the individual volumes to disk. Image stacks were acquired with isotropic voxels at a resolution of 1.24 μm × 1.24 μm × 1.24 μm per voxel.

2.5. Reconstruction

After the scanning procedure, the data consisted 28 512 × 512 image stacks per physical section, each containing 100 optical slices. In this scenario each brain slice data contained 2800 images, and the total number of acquired images for the seven tissue slices was 19,600. Due to the minor inaccuracy of the motorized stage, the image stacks had to be realigned to prevent overlapping and visible seams. To accomplish this each image stack was converted from the native fluoview tiff stack format to a tiff image series using imaging software (ImageJ, NIH). Next, the Volume Integration and Alignment System (Vias, CNIC, Mt. Sinai School of Medicine) was used to align and recombine the stacks. The alignment was initially performed on individual physical sections; the 28 image stacks were manually aligned using Vias' toolset. After each individual slice was reconstructed, the seven newly created data sets from the physical slices were aligned and merged using the third ventricle and optic chiasm as alignment cues in the tissue sections. The final 8-bit volume resolution of the reconstructed mouse vasopressin system was 3508 × 2072 × 700, which represents just less than 5 gigabytes of total data.

2.6. Rendering

Amira (TGS), Volsuite (Ohio Supercomputing Center) and custom written visualization software were used to stereoscopically render the dataset in realtime. Due to the size of the dataset, volume rendering on commodity hardware was difficult, and required the use of specialty data formats and rendering hardware. More specifically, the raw data was converted into Amira's large disk data format that permits access to data larger than can be loaded in memory, and is paged as necessary. Once access to the data had been established, a VolumePro 1000 (TeraRecon) hardware volume rendering board and a 4-node imaging cluster were utilized to visualize the data. Utilizing maximum intensity projection, as well as color and opacity maps, the hypothalamic data was rendered in an interactive environment permitting real-time clipping and modification of rendering parameters. Volsuite (Ohio Super Computing Center) and custom written software was also used to render volumes of interest from within the data in stereoscopic 3D.

3. Results

Utilizing the described staining procedure the vasopressin system was clearly stained and provided a bright fluorescent signal. The long incubation times permitted full penetration of the antibody through the thick 200 μm tissue sections and this was evidenced by no reduction in intensity through the image stacks along the *z*-dimension. As expected, the 200 μm tissue sections shrank in the *z*-dimension when dried on the slide to approximately 62% of the original thickness. Immuno-positive cell bodies were clearly visible in the PVN, SCN and SON, as previously reported (Burford et al., 1974). Stained fibre tracks were seen to terminate on the intensely stained median eminence where the neurohormone is released (Verbalis et al., 1986). Fig. 1 displays the tiled images from the seven physical slices used to generate a 3D map of the mouse vasopressin system.

Each of the seven images is a *z*-projected stack comprised of 2800 512 × 512 optical sections aligned and recombined. Fig. 2

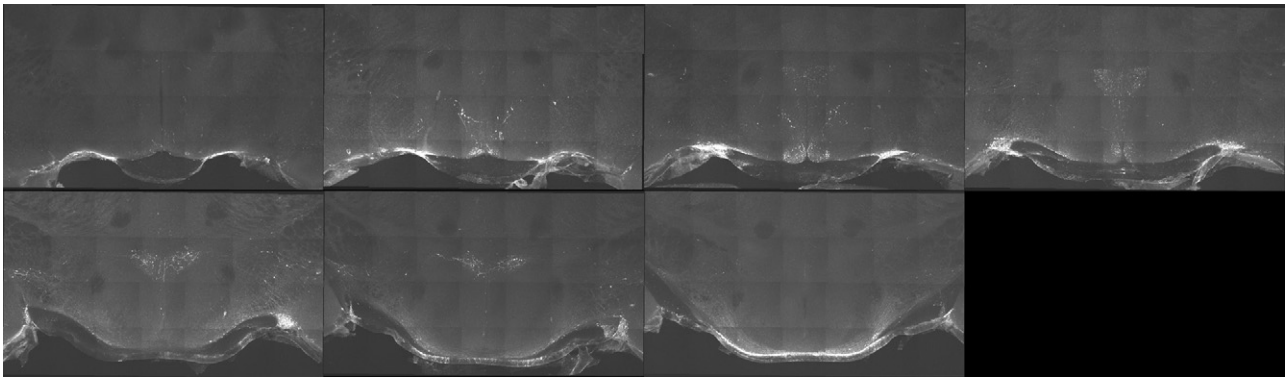

Fig. 1. The above images are *z*-projected confocal stacks from each of the seven 200 μm physical slices immuno-positive for vasopressin. Imaged tissue sections are organized with the four most rostral sections in the top row and the three most caudal sections on the bottom row. Each image is generated by recombining the tiles from 28 microscopic fields per slice. The dimensions of each tissue image stack are 3508 × 2072 × 100 with a resolution of 1.24 μm per pixel. Individual cell bodies are discernible as well as the macrocellular structure of the vasopressin neuroendocrine network.

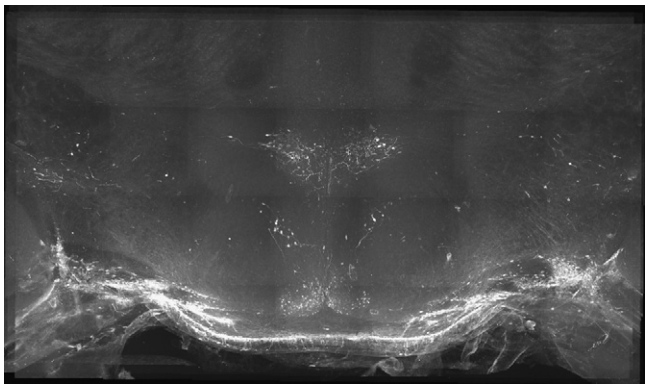

Fig. 2. This image is a *z*-projected representation of the entire mouse vasopressin system including 700 optical sections from the 7 realigned tiled physical slices. This image is a composite of 19,600 individual optical sections from 196 20× microscopic fields, and is approximately 5 gigabytes in size.

depicts the entire data volume and is a *z*-projected image of the seven axially aligned physical slices. Cell groupings and fiber tracts that make up the hypothalamic vasopressin system are clearly visible with subcellular resolution. Fig. 3 displays an expanded portion of the data in higher resolution depicting the suprachiasmatic nuclei (SCN). Numerous vasopressinergic cell bodies are visible within the SCN. This figure is a stereoscopic image, and can be visualized three dimensionally using the cross-eyed viewing method. Correctly viewing the image in stereoscopic 3D allows the depth of the volume data to become apparent as well as relationships between the different cellular layers in and around the SCN. Numerous vasopressinergic cell bodies are visible within the SCN. Fig. 4 is an image representative of the entire vasopressin system volume rendered using a mean intensity function and applied color map. Volume rendering the entire mouse vasopressin system allows a view of the hypothalamus previously unseen. This image represents a fluorescently stained piece of tissue measuring 4.35 mm × 2.6 mm × 1.4 mm with the preservation of individual cellular structure and a resolution of 1.2 μm per voxel.

4. Discussion

High resolution multi section confocal imaging provides data sets that generate otherwise impossible views of physiological phenomena. Here, we document an example focusing on the hypothalamus in the male mouse. We created a 3D map of the mouse vasopressin system highlighting the major cell groupings

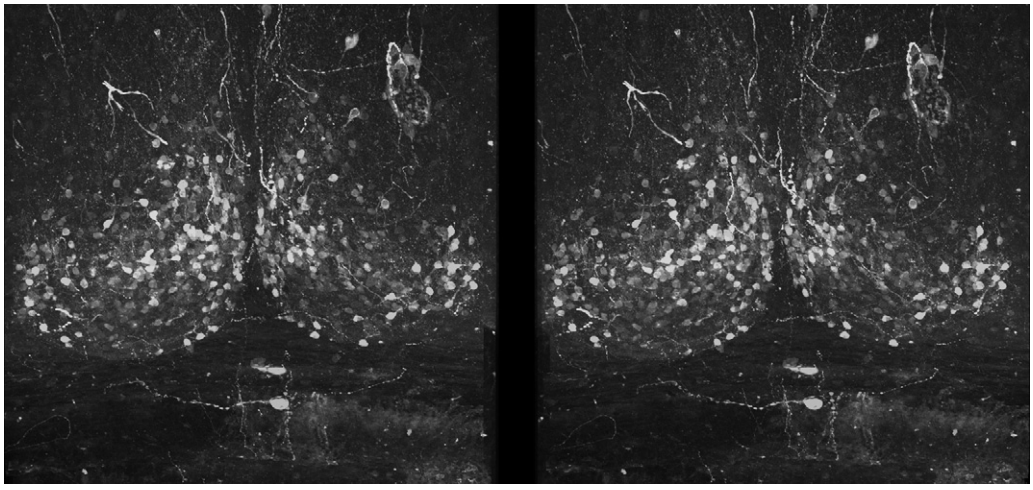

Fig. 3. This is a stereoscopic image of the suprachiasmatic nuclei (SCN) with visible vasopressinergic cell bodies. The image is a small portion of the actual data from the reconstructed AVP system as seen in Fig. 2. This image gives an idea of the magnitude and depth of the acquired data and is still less than 25% of full resolution. Use the cross-eyed viewing method to see the image in stereoscopic 3D. Stare at the point between the two images and slowly cross your eyes until they merge into a center image. The use of stereoscopic projection techniques permits insights into the data not available in 2D viewing; spatial relationships between different cell layers and neural tracts are easily identified.

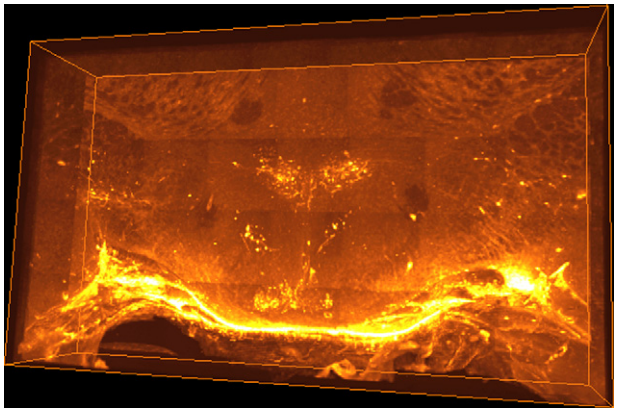

Fig. 4. This is an image of the mouse vasopressin system data volume rendered in our interactive stereoscopic environment. The rendering uses a maximum intensity projection with a colormap to highlight the data. The dimensions of the data are $3508 \times 2072 \times 700$ with a pixel resolution of 1.24 μm. The object can be interactively rotated, clipped, re-colored and zoomed.

and connections that make up this elaborate network. The successful application of this method is associated with a number of factors that must be addressed including slice thickness, antibody penetration, acquisition time, photo-bleaching, brightness inhomogeneities, data re-alignment and size.

The use of thick tissue sections for reconstruction is beneficial on a number of levels. Firstly, the fewer the number of tissue slices, the less perturbations and destructive artifacts due to tissue processing are incurred. By using 200 μm tissue sections, more cell layers are preserved in their natural state reducing the number of transected cells that negatively affect data set accuracy. Secondly, by using fewer tissue slices, the amount of data processing required to generate the final volume is minimized. More specifically, the effort to digitally co-register image stack tiles and *z*-align the individual reconstructed tissue slices is reduced. Preliminary experiments in our lab indicated that the use of such thick tissue sections required relatively long incubation times with the antibodies for successful penetration through the tissue. It was established that 72 h in the primary antibody and 48 h in the secondary antibody was sufficient time for total antibody penetration. This was evidenced by a lack of reduction in intensity of the acquired image stacks in the *z*-dimension. When three dimensionally imaging such a large area of tissue, the data acquisition time must also be taken into account. In our imaging system, to capture a $512 \times 512 \times 100$ matrix of confocal data using a high quality scan takes 4 min 31 s. We acquired 196 such image stacks with a total scanning time of 14 h and 42 min to acquire all the data. This was the actual scanning time and does not include saving the stacks, moving the stage and setting up the imaging system. Initially, we wanted to acquire image stacks at $1024 \times 1024 \times 200$, doubling the pixel resolution to 0.621 μm, but acquisition time and data size were prohibitive in such a scenario; both would increase by a factor of 4. Longer imaging times can also cause photo-bleaching to become more of a problem. Confocal imaging typically causes less bleaching than brightfield microscopy due to a single point light source rather than field wide illumination; consequently, we observed little to no bleaching during our ~5 min scan period. However, when increasing the acquisition time this issue must be taken into account, and the use of anti-bleaching mounting media (such as Vectashield) positively affects this outcome.

Another source of data error is brightness inhomogeneities caused by differential field illumination. Each microscopic field was illuminated non-uniformly and when the image stacks were tiled, square blocks of data are visible. Specifically, the top right corner of each tile is approximately 7% dimmer than the rest of the image; this is typically attributed to obstacles in the path of peripheral rays and variance in detection efficiency in the microscopic field (Model, 2002). This is common in many microscopic imaging systems and could not be overcome in our experiment. However, we are working on implementing an automated corrective algorithm that overcomes this issue through the generation of a background corrective image to apply to the tiles and correct for such inconsistencies. When using a maximum intensity projection the inhomogeneities disappear (or are greatly reduced), and are most visible on the background of each data slice. Consequently, this did not greatly affect the final tissue reconstruction, but may have affected the automated alignment procedure. The alignment protocol was first performed on each physical slice, and then to *z*-align each of the seven slices. The automated algorithms provided in Vias failed on numerous occasions, this required manual alignment of the 196 stacks and alignment of the seven physical slices. Alignment in all three planes dictates that the data have similar features, landmarks, or a portion of overlapping data. Alignment in the *XY* planes was accomplished by having a small pixel overlap in the image tiles, making alignment relatively simple by using adjacent matching pixels as the reference points. Alignment in the *z*-dimension was slightly more difficult and necessitated the use of physical landmarks since no overlapping data could be referenced. In the current model, the 3rd ventricle and optic chiasm were sufficient for adequate re-alignment.

The final issue we observed when creating this reconstruction was the magnitude of the acquired data. The microscopic image data was extremely large and included 19,600 images which needed to be processed a number of times for each step in the reconstruction. We decided to convert the images from 16 bit to 8 bit shading to immediately reduce the size by 2 without any adverse visual effects on image quality. Images from the acquisition software actually contain only 12 bit per pixel stored in a 16 bit image, so the net effect on image quality was limited. Pre-processing steps also required that we convert each of the 196 multi-tiff images to an image sequence for the re-alignment software. Wherever possible we automated procedures, but each step did require intervention. The final tissue volume was $3508 \times 2072 \times 700$ pixels and approximately 5 gigabytes in size. Working with a single piece of data this large is cumbersome on a desktop PC and it is necessary to utilize a machine with 64-bit architecture capable of addressing more than 2 GB of memory space, or a small networked cluster. Once the volume was generated we faced the further problem of stereoscopically visualizing the data in an interactive environment.

In order to volume render the data, a method that displays the composite of 19,600 images at a single time, we used a number of imaging systems including a mini visualization cluster, a hardware-based rendering card and custom software using downsized and chunks of data. The small visualization cluster was a linux (gentoo) based graphics cluster with four nodes each with individual graphics processing units (GPUs). Once configured the cluster performed well, using a sort-first rendering scheme (Hansen et al., 1997) whereby each node rendered 1/4 of the final display image that were composited on the head nodes' display using the remote frame buffer protocol. Usage of the cluster included an initial overhead setup time as well as the usage of a gigabit local area network to transfer the rendered tiles. This system was able to render the data in passive (side-by-side) stereo images, however it was unable to project active stereo images (using liquid crystal shutter glasses). The usage of the Terrarecon hardware volume rendering board permitted an active stereo rendered image, but required the conversion to an arbitrary data format used by Amira: large disk data. Also, this system was hampered by long load times (>8 min) due to the low bandwidth of the PCI interface, but nevertheless provided an interactive stereoscopically rendered visualization of the entire volume. We also rendered smaller regions of interest in the data

using custom written software. This provided clean and interactive viewing on desktop based PC's with high frame rates. We are currently in the process of generating software capable of using level of detail rendering (LOD) techniques (Weiler et al., 2000) that will allow the visualization of such data on commodity desktop PC's using intelligent data management routines. Using this technique suits the current data well since the resolution is such that it would be difficult to display the image in full detail without using a high resolution display wall. Most desktop screens do not approach 3500×2070 pixels and full data set detail can only be imaged when zooming in to the data. It should also be noted that no attempt was made to correct for the tissue shrinkage in the *z*-dimension. This was in order to maintain isotropic voxels, however this parameter is easily modified during volume rendering and will most likely be incorporated into our LOD rendering system.

The power of visualizing these data sets in stereoscopic 3D is also notable, as indicated by Fig. 3 and shown to be beneficial in other stereoscopic atlases (Clements and Blank, 2008). If the viewer is able to successfully recombine the two viewpoints into a 3D representation, and compare this to looking at one of the monoscopic images, the difference is clear. The stereo-image provides details and features regarding spatial structure not apparent in the two-dimensional image. In particular, the arrangement of the cells around the central core of the SCN is clearly visible. Neuronal systems particularly benefit from such display paradigms due to the inherent 3D structure that is frequently overlooked in neuroscience research. Indeed, a better knowledge of spatial relationships of hypothalamic nuclei should help analyze and interpret studies disrupting these connections (Young and Stanton, 1991).

The use of the current technique for the generation of interactive brain mapping data is in contrast to current atlases. Firstly, it is designed to create very detailed views of 3D subcellular architecture and preserve macrostructure of overlying neuronal networks. The display of the volume is also a departure from many current reconstructions (Bertrand and Nissanov, 2008; Hjornevik et al., 2007), since it is the actual microscopic fluorescent images that are displayed rather than a surface mesh generated by segmentation or thresholding. While the latter approach is a valid form of visualization, can require much less computing power and can be beneficial for calculating volumetric measurements of hypothalamic structures (Scallet and Meredith, 2002), subtle details are lost in the data. This is because surfaces typically contain a single value rather than a range of intensities, creating rapid transitions between adjacent structures that may otherwise be graded changes.

In conclusion, we have generated a high resolution microscopic reconstruction of the immunoreactive vasopressin system in the male mouse brain. The data includes a volume of tissue that measures $4.35\,\text{mm} \times 2.6\,\text{mm} \times 1.4\,\text{mm}$ with a voxel resolution of $1.2\,\mu\text{m}$. The data set size is just less than 5 gigabytes and is a composite of 196 microscopic fields including 19,600 optical sections. The reconstruction provides volume rendered stereoscopic views of this neuronal system that otherwise could not be seen using current technology. Data of this type will enhance our understanding of the contribution of structure to function, and provide detailed information regarding neuronal connectivity and cellular distribution. With the use of multiple concurrent fluorescent stains relationships between cell phenotypes can be deciphered and structural differences can be associated with behavioral and/or disease associated changes. The volumetric data can be further exploited for virtual bioinformatics experiments, assessing signal propagation/conduction and how neural network function changes with modified structure. Our research group intends to refine the protocol using a 4 pi 2-photon microscope as well as multiple concurrent stains to generate a neurochemical interactive volume of the entire neuroendocrine hypothalamus. This will include all hormones produced in the structure to provide an informative 3D atlas with submicron resolution that preserves individual cellular 3D structure. More information and media can be accessed at http://bioweb.biology.kent.edu/FacultyPages/Clements/vasopressin.html.

References

Bertrand L, Nissanov J. The neuroterrain 3D mouse brain atlas front. Neuroinformatics 2008;2:3.

Birkfellner W, Figl M, Matula C, Hummel J, Hanel R, Imhof H, et al. Computer-enhanced stereoscopic vision in a head-mounted operating binocular. Phys Med Biol 2003;48:49–57.

Burford GD, Dyball REJ, Moss RL, Pickering BT. Synthesis of both neurohypophysical hormones in both the paraventricular and supraoptic nuclei of the rat. J Anat 1974;117:261–9.

Caldwell HK, Lee HJ, Macbeth AH, Young III WS. Vasopressin: behavioral roles of an "original" neuropeptide. Prog Neurobiol 2008;84(January (1)):1–24 [Epub November 4, 2007].

Clements RJ, Blank JL. A stereoscopic volume rendered brain atlas. Brains Minds Media 2008;3:1–9.

Hansen C, Krogh M, Painter J. Parallel rendering techniques for massively parallel visualization. In: 2nd AIZU international symposium on parallel algorithms architecture synthesis (pAs '97); 1997. p. 276.

Hjornevik T, Leergaard TB, Darine D, Moldestad P, Dale AM, Willoch F, et al. Three-dimensional atlas system for mouse and rat brain imaging data front. Neuroinformatics 2007;1:4.

Liao WH, Agarwal SJ, Aggarwal JK. The reconstruction of dynamic 3D structure of biological objects using stereo microscopes. Mach Vis Appl 1997;9:166–78.

Liu S, Weaver DL, Taatjes DJ. Three-dimensional reconstruction by confocal laser scanning microscopy in routine pathological specimens and malignant tumors of the human breast. Histochem Cell Biol 1997;107:267–78.

McCormick SD, Bradshaw D. Hormonal control of salt and water balance in vertebrates. Gen Comp Endocrinol 2006;147(May (1)):3–8 [Epub February 2, 2006].

Model MA. Calibration and shading correction for fluorescence microscopes. Curr Protoc Cytomet 2002 [update in 2006; unit 10–14].

Orban GA, Janssen P, Vogels R. Extracting 3D structure from disparity. Trends Neurosci 2006;29(8):466–73.

Perry J, Kuehn D, Langlois. Teaching anatomy and physiology using computer-based stereoscopic images. J Coll Sci Teach 2007:18–23.

Scallet AC, Meredith JM. Quantitative three-dimensional reconstruction: feasability for studies of sexually dimorphic hypothalamic development in rats. Neurotoxicol Toxicol 2002;24:81–5.

Sheen NJL, Morgan JE, Poulson JL, North RV. Digital stereoscopic analysis of the optic disc. Evaluation of a teaching program. Ophthalmology 2004;111:1873–9.

Smith JR, Connel SD, Swift JA. Stereoscopic display of atomic force microscope images using anaglyph techniques. J Microsc 1999;196:347–51.

Stricker EM, Verbalis JG. Water intake and body fluids. In: Fundamental neuroscience. San Diego, CA: Academic Press; 1999. pp. 1111–26.

Thomsen MN, Lang RD. An experimental comparison of 3-dimensional and 2-dimensional endoscopic systems in a model. J Arthrosc Rel Surg 2004;20(4):419–23.

Verbalis JG, Baldwin EF, Ronnekleiv OK, Robinson AG. In vitro release of vasopressin and oxytocin from rat median eminence tissue. Neuroendocrinology 1986;42:481–8.

Weiler M, Westermann R, Hansen C, Zimmermann K, Ertl T. Level-of-detail volume rendering via 3D textures. In: Symposium on volume visualization; 2000. p. 7–13.

Young JK, Stanton GB. A three-dimensional reconstruction of the rat hypothalamus. Brain Res Bull 1991;26(2):279–83.